ELSEVIER

Journal of Molecular Catalysis A: Chemical 175 (2001) 91–103

JOURNAL OF MOLECULAR CATALYSIS A: CHEMICAL

www.elsevier.com/locate/molcata

Characterization and evaluation of the nature of chemical species generated in hybrid Ziegler–Natta/metallocene catalyst

Maria Madalena de Camargo Forte [a,*], Fernanda Vieira da Cunha [a], João Henrique Zimnoch dos Santos [b]

[a] *UFRGS, Escola de Engenharia, Laboratório de Materiais Poliméricos, r. Osvaldo Aranha, 99-Porto Alegre 90035-190, Brazil*

[b] *UFRGS, Instituto de Química, Av. Bento Gonçalves 9500, Porto Alegre 91501-970, Brazil*

Received 25 September 2000; received in revised form 4 January 2001; accepted 15 March 2001

Abstract

In the present work $CpTiCl_3$ pretreated with tri-*iso*-butylaluminium was immobilized on $MgCl_2$ supported Ziegler–Natta catalyst. The resulting catalysts were characterized by a series of techniques, namely thermal analysis (TGA/DTA), X-ray photoelectron spectroscopy (XPS), ^{27}Al magic angle spin nuclear magnetic resonance (^{27}Al MAS–NMR), UV–VIS spectroscopic analysis, inductively-coupled plasma–atomic emission spectroscopy (ICP–AES) and elemental analysis. The catalysts UV–VIS spectrum showed a broad absorption band at 390 nm indicating the presence of metallocene cyclopentadienyl ring. According to XPS analysis, only hybrid catalysts showed two peaks in the Ti ($2p^{3/2}$) region after the spectrum deconvolution, a lower binding energy peak at 455 eV and another one at 457 eV (Ti^{4+}). These appear to be due to difference of electronegativity in the coordination sphere of the Ti due to the $TiCl_4$ and the Cp(*i*-Bu)$TiCl_2$ fixed on the hybrid Ziegler–Natta catalyst. All catalyst systems were active in ethylene-1-butene copolymerization. The resulting polymers obtained with the hybrid catalyst showed a shoulder in the DSC thermogramme fusion peak. It might be caused by a polymer fraction produced by the additional Ti center in the catalyst due to the Cp(*i*-Bu)$TiCl_2$. Microscopic analysis showed that the polymer replicated the spherical morphology of the catalyst grain.

Keywords: Hybrid catalysts; Ziegler–Natta; Metallocene; XPS; UV–VIS; Ethylene copolymer

1. Introduction

The nature of the active centers presented in the stereospecific Ziegler–Natta catalysts has been largely studied in the literature [1–7]. Most of these works deal with systems where titanium tetrachloride ($TiCl_4$) was supported on magnesium dichloride ($MgCl_2$) in the presence of an internal electron donor. Busico et al [4–7], in a series of papers, proposed the existence of two types of active sites depending on the support face acidity, Ti_2Cl_6 being the stereospecific one responsible for the isotactic chain propagation, while $TiCl_3$ the nonsterospecific one responsible for the random propagation [1–7], as shown in Scheme 1. Catalyst activity depends on the activation by alkyl aluminium co-catalyst, such as trimethylaluminium (TMA), triethyaluminium (TEA) and tri-*iso*-butylaluminium (TIBA).

In the 1980s, Sinn and Kaminsky discovered a new class of homogeneous stereospecific catalysts, combining group 4 metallocene compounds with methylaluminoxane (MAO), capable of polymerizing

* Corresponding author.

1381-1169/01/$ – see front matter
PII: S1381-1169(01)00172-8

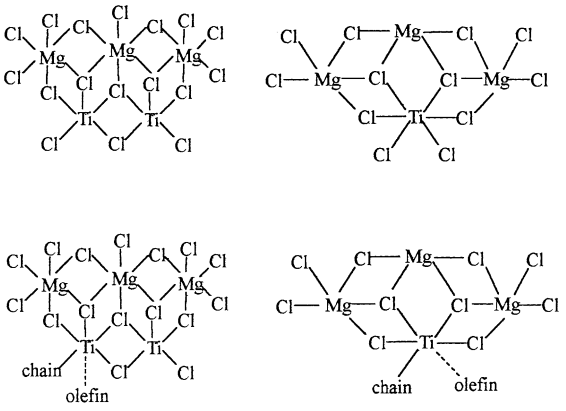

Scheme 1.

α-olefins in high activity. Metallocene catalysts have been constantly reviewed in the literature [8–11].

In the metallocene catalytic systems, there is only one type of active center with defined coordination sphere (single site catalysts). Some proposals of active center formation between the metallocene and MAO are reported in the literature [12,13]. Unfortunately, these catalysts require a large amount of expensive MAO to reach the maximum catalytic activity, which, to some extent, may impair its value in commercial applications. For that reason, much effort has been made not only to lower the amount of MAO in polymerization but also to find a new co-catalyst to replace it [14–17]. Moreover, besides the high amount of MAO, there are other disadvantages in the use of soluble metallocene catalysts. A solution polymerization process requires separation of the polymer recovery and purification of the solvent. On the other hand, gas phase processes have lower cost and energy consumption. Most of the existing slurry and gas-phase polymerization plants run with heterogeneous catalysts [18–21], therefore homogeneous catalysts must be heterogenized if there will be application in those processes. Moreover, the heterogenization of metallocene is necessary to avoid reactor fouling with finely dispersed polymer particles and to produce polymer particles with controlled morphology [22,23].

In the last decade, many attempts have been made in the heterogenization of metallocene compounds. Different preparatory routes are described in the literature [24–26] aimed at developing supported metallocene catalysts which could substitute, without higher costs, the heterogeneous catalyst Ziegler–Natta ($TiCl_4/MgCl_2$) in the industrial plants.

Metallocene catalysts are capable of producing polymers with special properties depending on the organometallic precursor employed. The linear low density polyethylene (LLDPE) produced by the copolymerization of ethylene with α-olefins is obtained by metallocene catalyst/MAO system, with homogeneous distribution of the comonomer in the polymer chain. The production of polymers with narrow molecular weight and composition distribution leads to many improvements in physical properties, such as clarity, impact resistance and environment crack resistance. However, such polymers, besides presenting a higher tendency to melt fracture, are much more difficult to be processed. Therefore, molecular weight distribution and composition distribution broadening is desirable for certain applications. One approach to overcome such inconvenience consists of concomitantly using two catalysts with different responses to hydrogen and comonomer in the same reactor for producing polymers with broad molecular weight distribution. A few reports in the literature deal with the immobilization of two metallocene catalysts on the same support. For instance, $Et(Ind)_2ZrCl_2$ and Cp_2HfCl_2 grafted together on silica produce unimodal and bimodal polyethylene [27]. Broadening on polydispersion was also observed in polymers produced by zirconocene differing in the coordination sphere and co-supported on silica, such as $Me_2C(Cp)(2,7\text{-}(t\text{-}Bu)_2Flu)ZrCl_2$ and $Ph_2C(Cp)FluZrCl_2$ [28] or $Me_2Si(2\text{-}MeInd)_2ZrCl_2$ and $Me_2C(Cp)(Flu)ZrCl_2$ [29]. Very recently, Ziegler–Natta/metallocene hybrid and mixed catalysts have been employed for controlling the molecular weight distribution in polyethylenes [30]. Polyethylene bimodal was also achieved using a mixture of Ziegler–Natta catalyst and metallocene/MAO ones [31].

In previous work, we have studied the immobilization of zirconocene directly on silica support [32–34], on organosilicon-modified silica [35] and on hybrid sol–gel synthesized silica [36]. In the present work, we studied the immobilization of monocyclopentadienyltitanium trichloride ($CpTiCl_3$) pretreated with TIBA on $TiCl_4/DIBP/MgCl_2$ to obtain a hybrid

Ziegler–Natta/metallocene catalyst. The resulting catalysts were characterized by elemental analysis, X-ray photoelectron spectroscopy (XPS), inductively-coupled plasma–atomic emission spectroscopy (ICP–AES), thermal gravimetry analysis (TGA), UV–VIS spectroscopy and ^{27}Al magic angle spin nuclear magnetic resonance (MAS–NMR). The catalyst systems were evaluated in ethylene-1-butene copolymerization. Resulting copolymers were characterized by melting flow index (MFI), Fourier transformed–infrared spectroscopy (FT–IR) and differential scanning calorimetry (DSC). Catalyst and polymer morphology were analyzed by optical microscopy.

2. Experimental

2.1. Chemicals

All the chemicals were manipulated using the Schlenk technique. A fourth generation Ziegler–Natta catalyst with approximately 2.2 wt.% Ti and around 12 wt.% di-*iso*-butylphthalate (DIBP) (MCM1, Akzo Nobel Chemicals Inc.) and $CpTiCl_3$ (Bouder Scientific Company) were used as received. The alkyl aluminium compounds, TEA and TIBA (Akzo Nobel Chemicals Inc.) were employed in *n*-hexane solution. The *n*-hexane (IBRASOL) used in the catalyst preparation and copolymerization reactions was dried with 3 Å molecular sieve.

2.2. Catalyst preparation

Dry *n*-hexane (8 ml) was added into a Schlenk tube containing $CpTiCl_3$ (1 mmol), followed by dropwise addition of 0.7 ml of TIBA (2.8 mmol) under magnetic stirring. After 2 h at room temperature, the solution turned dark purple, nearly black, then it was added to a suspension of Ziegler–Natta catalyst (2 mmol of Ti) in *n*-hexane, in a glass reactor equipped with mechanical stirring. The mixture was kept at 40°C for 5 h at 300 rpm. The residual solid was washed with *n*-hexane and dried in nitrogen flow. The resulting catalysts metallocene/Ziegler–Natta hybrid catalysts (Met/ZN) were prepared with molar ratio between 0.2 and 0.5. For XPS comparative evaluation, two other catalysts were prepared under the same procedure as the hybrid ones, but in absence of the metallocene catalyst (ZNT1 and ZNT2).

2.3. Catalyst characterization

2.3.1. Elemental analysis

The catalysts were attacked by H_2SO_4 (2N) solution and the titanium content in it was determined by the colorimetric method with H_2O_2. The magnesium content was determined by titration with EDTA, while chloride content was determined by the Volhard method. The total organic content of the catalysts (residual ethanol, internal donor and aluminium compound) was assumed as the difference between 100 and the sum of the percentage of Ti, Mg and Cl.

2.3.2. X-ray photoelectron spectroscopy

XPS were obtained on a PHI 5600 Esca System (Φ Physical Electronics), using an Al monochromated 2 mm filament (Al Kα radiation, 1486.6 eV). Spectra were run at room temperature in low resolution (pass energy 235 eV) in the range of 1000–0 eV, and in high-resolution (pass energy 23.5 eV) modes for the Mg (2s), Al (2p) and Ti ($2p^{3/2}$) regions.

The solid catalyst samples were fixed on an adhesive copper tape as thin films. Prepared samples were then evacuated at 10^{-6} Torr by a turbo molecular pump in an introduction chamber for 90 min. During data collection, the ion pumped mass chamber was maintained at under vacuum less than 10^{-9} Torr. Each sample was analyzed at a 75° angle relative to the electron detector. Normally 50 scans were signal averaged for selected binding energy windows and processed by the software supplied by the manufacturer. Neutralizer environment was 21.5 mA.

Binding energies examined (element, transition, approximative binding energy, and range scanned) were as follows: Mg 2s, 89 eV, 100–85; Al 2p, 72.9 eV, 70–80; Ti $2p^{3/2}$, 454, 450–470; Cl $2p^{3/2}$, 199, 190–205; O 1s, 531, 525–540 eV; C 1s, 285, 280–292 eV. Accurate binding energy was determined by referencing to the Mg 2p core level from $MgCl_2$.

Estimation of surface atomic ratios involved integrated areas and calculated atomic sensitivity factors. The sensitivity factors employed were Mg (2s), 50.54; Al (2p), 57.59; Ti (2p), 347.0; Cl (2p), 152.6; O (1s), 136.5; C (1s), 58.2, empirically derived for the electron energy analyzer supplied by Perkin-Elmer.

2.3.3. Inductively-coupled plasma–atomic emission spectroscopy

The Al and Ti contents in the catalyst were also measured by ICP–AES on a Seiko spectrometer (SPS 7700). The catalyst samples were previously attacked by acid digestion using H_2SO_4 2N solution.

2.3.4. Thermal gravimetry analysis

The TGA analysis of the solid catalysts were performed in the TA instruments Universal model V1.7F equipment under N_2 atmosphere. Samples were heated from 30 to 1000°C at a heating rate of 20°C/min.

2.3.5. UV–VIS spectroscopy

The solid catalysts were characterized as slurry in Nujol. The analysis were performed in a DW-2000 spectrometer (Sim-Aminco, USA), equipped with a tungsten (vis) and deuterium (UV) lamps, and a beam scrambler, which diffuses the entering light to form a uniform field of illumination, eliminating any spatial differences between beams. In order to increase the transparency of the samples and the viscosity of the milieu, the solids were mixed with Nujol to form a slurry. All the samples were prepared in a glove box. The absorption spectra were recorded, under dry N_2 between 250 and 650 nm. Quartz cells (1.0 cm path length) were employed. Nujol was employed as reference. Soluble systems were analyzed by means of a Shimadzu spectrometer, UV-1601pcs in the 300–600 nm wavelength range using a quartz cell (1.0 cm path length), attached to a Schlenk flask as described in the literature [37].

2.3.6. Magic angles spin–nuclear magnetic resonance

MAS solid nuclear magnetic resonance (NMR) spectra were recorded by a Varian 400 MHz spectrometer operating at 104.3 MHz for ^{27}Al. Peak positions were relative to external $Al(NO_3)_3{\cdot}9H_2O$ (^{27}Al). Prior to the spectra recording the catalyst samples were transferred into zirconia spinner in a glovebox.

2.4. Polymerization reactions

Ethylene-1-butene copolymerization reactions were carried out in 1 dm^3 of hexane in a 2 dm^3 Büchi reactor equipped with mechanical stirring and temperature control. The reactions were performed at 75°C for 2 h under 7 bar of pressure. Hydrogen (0.35 g) was used in all reactions. The employed Al/Ti molar ratio was 200 or 1000. The components were added into the reactor in the following order: solvent, TEA, catalyst, comonomer, hydrogen and ethylene. Each polymerization reaction was repeated at least three times under identical conditions, in order to have three runs with catalyst activity differences lower than 10%.

2.5. Polymer characterization

The comonomer incorporation was evaluated by infrared techniques, using a Nicolet 710 FT–IR spectrometer, where the polymer was analyzed as film samples. The MFI was determined in a Tinius Olsen MP 987 extrusion plastometer at 190°C, using a 2.16 kg charge. The intrinsic viscosity in decahydronaphthalin at 135°C was determined using a SOFICA-CINEVISCO viscosimeter. Copolymer melting points and crystallinity were determined on a DuPont DSC 2910 differential scanning calorimeter connected to a thermal analyst 2100 integrator. The analysis were performed at a heating rate of 10°C/min. Catalyst and polymer morphology were analyzed by an optical microscope Zeiss coupled to 545 polaroid model MC 63C.

3. Results and discussion

In this work, a fourth generation Ziegler–Natta catalyst was used with the aim of introducing a new titanium species in it, such as metallocene ones. So a hybrid catalyst could be obtained by modifying the first one. The fourth generation Ziegler–Natta catalyst is a $TiCl_4$ catalyst supported on $MgCl_2$ (DIBP as the internal electron donor) with a spherical morphology.

The metallocene compound $CpTiCl_3$ was previously treated with TIBA compound in order to get it in an appropriate form for better interaction with the Ziegler–Natta catalyst. The reaction between $CpTiCl_3$ and TIBA leads to an alkylated titanium soluble compound ((Cp)(*i*-Bu)$TiCl_2$) which favors its interaction or immobilization on $MgCl_2$ faces. The immobilization of this titanium compound with a cyclopentadienyl ring and *iso*-butyl group introduces a new type of potential active center in the Ziegler–Natta catalyst.

Table 1
Elemental analysis results, Ti, Cl and Mg content for catalysts with different Met/ZN molar ratio

Catalyst	Met/ZN molar ratio	Cl (%)	Mg (%)	Ti (%)	Other (%)[a]
Ziegler–Natta	–	58.6	18.7	2.2	20.5[b]
ZNM21	0.2	61.5	17.5	2.6	18.4
ZNM23[c]	0.28	57.7	15.6	2.6	24.1
ZNM22[c]	0.28	59.1	18.0	2.9	20.0
ZNM24[c]	0.5	55.7	14.8	3.0	26.5
ZNM20[c]	0.5	57.5	17.3	3.2	22.0

[a] Aluminium and organics (internal electron donor, alkylaluminium e metallocene).
[b] Organics (internal electron donor).
[c] The difference between the catalyst ZNM22/23 and ZNM20/21 was the catalyst lot preparation.

This new active center might modify the olefin polymerization performance and some polymer properties.

Table 1 displays the titanium, chlorine and magnesium contents for the different catalysts prepared in this work. The Met/ZN molar ratio reports the concentration of metallocene to Ziegler–Natta employed in the hybrid catalyst preparation. For comparative reasons, data from commercial Ziegler–Natta catalyst were also included. According to Table 1, an increase in the Met/ZN molar ratio results in an increase of the Ti content, suggesting that it could be due to the immobilization of the titanocene on the solid catalyst. Small differences in the values of Cl, Mg and Ti, for the same Met/ZN molar ratio, can be attributed to little differences in the Ziegler–Natta catalyst due to different commercial lots employed in hybrid catalysts preparation and analytical errors (such as acid digestion step, dilution, calibration curve).

Table 2 shows the results of elemental analysis of a hybrid catalyst (ZNM24), a Ziegler–Natta catalyst and two others Ziegler–Natta treated with alkyl aluminium (ZNT1 and ZNT2). From the XPS results, it can be observed that all the catalysts treated with alkyl aluminium presented Al in it, showing that there is a chemical interaction of this compound with the catalyst surface. The presence of aluminium in the catalysts treated with TIBA was also confirmed by ICP–AES analysis. The content of aluminium in the catalyst was proportional to the amounts of TIBA used in its preparation.

The ^{27}Al MAS–NMR analysis (Fig. 1) of the ZNM24 (hybrid) and ZNT1 catalysts, shows the same signals presenting the following chemical shift: around 10, 24, 68, 82, 105 and 143 ppm. Therefore, the chemical environment of the compound of alkyl aluminium is the same in all the catalysts, independent of the initial Met/ZN molar ratio, used in the preparation of those. The nature of the surface species seems to be very complex. When an alkyl aluminium, like TIBA, is added to a Ziegler–Natta catalyst, the aluminium compound reduces the $TiCl_4$ into $TiCl_3$ with its subsequent alkylation. Besides, the excess of TIBA in the metallocene solution used in the catalyst preparation reduces the $TiCl_4$ and removes the DIBP

Table 2
Elemental analysis of catalysts by XPS and ICP

Catalyst	XPS						ICP		
	C (%)	O (%)	Cl (%)	Mg (%)	Ti (%)	Al (%)	Ti (%)	Al (%)	Al/Ti molar ratio
ZNM24[a]	38.8	23.5	23.9	10.5	2.5	1.3	2.8	1.1	0.4
ZNT1[b]	43.9	24.5	17.1	8.1	1.1	5.2	2.6	2.0	0.8
ZNT2[c]	40.2	26.1	20.9	9.8	1.3	1.8	2.5	1.0	0.4
Ziegler–Natta	42.1	17.5	26.2	12.2	2.0	–	2.2	0.0	0.0

[a] Hybrid catalyst, Al/Ti molar ratio = 0.7; Met/ZN molar ratio = 0.5.
[b] Prepared as in a) Al/Ti molar ratio = 1.1, but in absence of metallocene coumpound.
[c] Prepared as in a) Al/Ti molar ratio = 0.7, but in absence of metallocene coumpound.

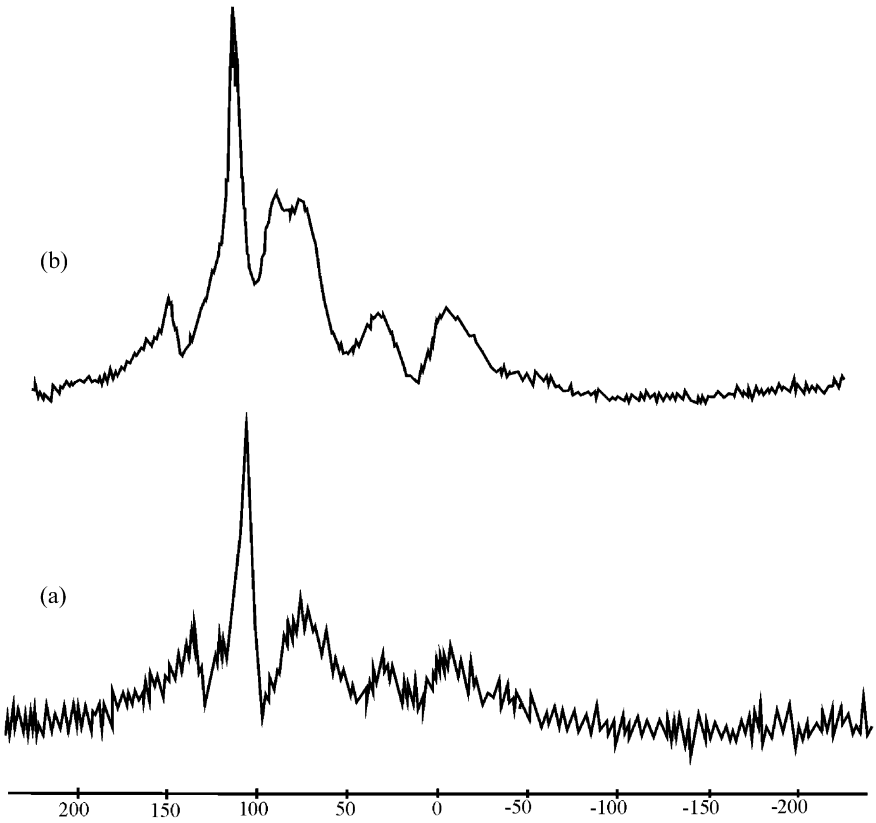

Fig. 1. ^{27}Al MAS–NMR spectra: (a) ZNT1; (b) ZNM24.

(internal donor) of the Ziegler–Natta catalyst. It can interact with the support in different ways [38,39]. Potapov et al, in a ^{27}Al NMR study of $TiCl_4/MgCl_2$ and $TiCl_4$/DIBP/$MgCl_2$ treated with trialkyl aluminium compound, verified that the main compound of aluminium in the catalyst surface is likely a dialkyl aluminium chloride. The chemical shifts were attributed mainly to the adsorption of Al(*i*-Bu)$_2$Cl on the $MgCl_2$ surface, produced in the metallocene alkylation and $TiCl_4$ reduction. The chemical shift at around 82 ppm might be attributed to the five-fold coordination with three *iso*-butyl groups as a dimer on the $MgCl_2$ (1 0 0) face as already described in the literature [40]. The other signals are still under investigation and can suggest that many other Al species are on $MgCl_2$ surface like a six-fold coordination of Al.

Table 3 displays Ti contents in the hybrid catalyst obtained with three different techniques, ICP–AES, colorimetric method and XPS. The values of the ICP–AES analysis and colorimetric method were more similar because, in both cases, the total amount of titanium is measured after its extraction from the catalyst by acid digestion. On the other hand, the analysis of XPS quantifies only the titanium present in the uttermost catalyst surface (ca. 3 nm). The results show that the titanium is exclusively in the surface of the catalyst as expected.

The commercial Ziegler–Natta and two hybrid catalysts were analyzed through TGA to evaluate their thermal stability (Fig. 2). For all the catalysts, a mass

Table 3
Comparison of the Ti content determined by ICP, colorimetry and XPS techniques

Catalyst	ICP	Colorimetry	XPS
Ziegler–Natta	2.2	2.2	2.0
ZNM24	2.8	3.0	2.5

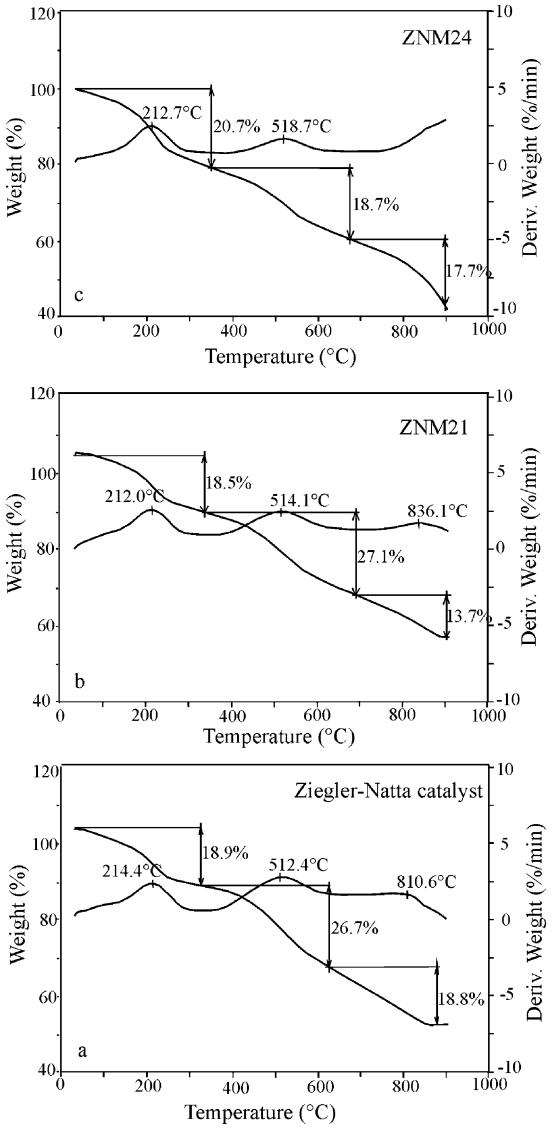

Fig. 2. TGA thermogrammes: (a) Ziegler–Natta catalyst; (b) ZNM21; (c) ZNM24.

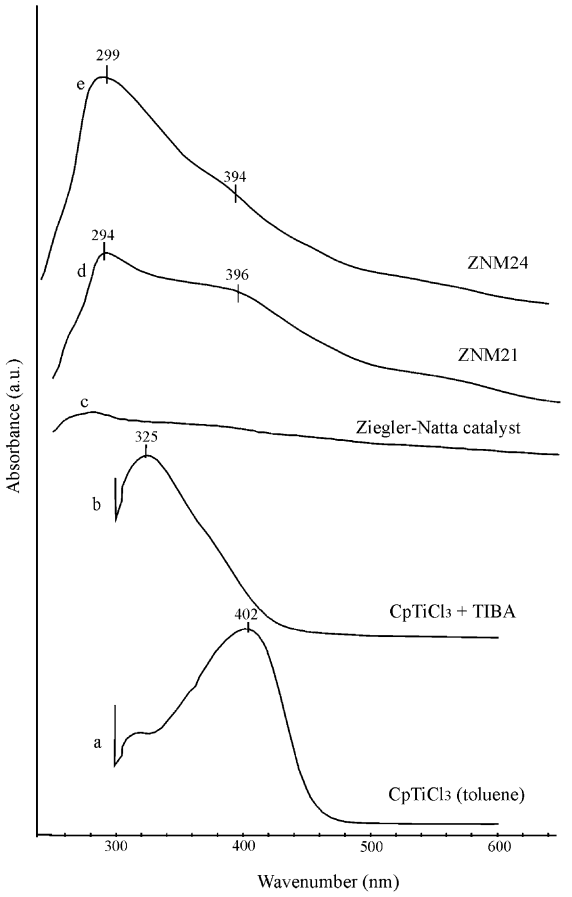

Fig. 3. UV–VIS spectra. (a) $CpTiCl_3$ 2×10^{-4} mol l^{-1}, in toluene; (b) $CpTiCl_3$ + TIBA, grafting solution; (c) Ziegler–Natta catalysts; (d) supported catalyst ZNM21; (e) supported catalyst ZNM24.

loss around 213°C was observed, attributed to an outlet of $TiCl_4$ from the crystalline $MgCl_2$ matrix, and a mass loss around 515°C that can be attributed to the internal donor loss, here DIBP, present in the Ziegler–Natta catalyst. This thermal behavior is in agreement with those already reported by Terano et al [41,42].

The soluble metallocene catalyst were analyzed by UV–VIS spectroscopy in toluene solution, while the hybrid catalysts spectra were obtained from a Nujol catalyst slurry carefully manipulated under controlled atmosphere. Fig. 3 displays the spectra of the different catalysts. The spectrum of the metallocene in toluene solution presents a maximum absorption at 402 nm, attributed to π–π^* transition of the Cp ring [43] (Fig. 3a). After TIBA addition, in the solid $CpTiCl_3$ compound, this band shows an hypsochromic shift to 325 nm (Fig. 3b). Similar behavior is reported in the literature in the case of the reaction of zirconocene with alkyl aluminium compounds. The hypsochromic shift was attributed to the formation of monoalkylated species [43]. Corroborating this observation, the shift from 402 to 325 nm under our experimental conditions can be also attributed to a monoalkylated titanocene species.

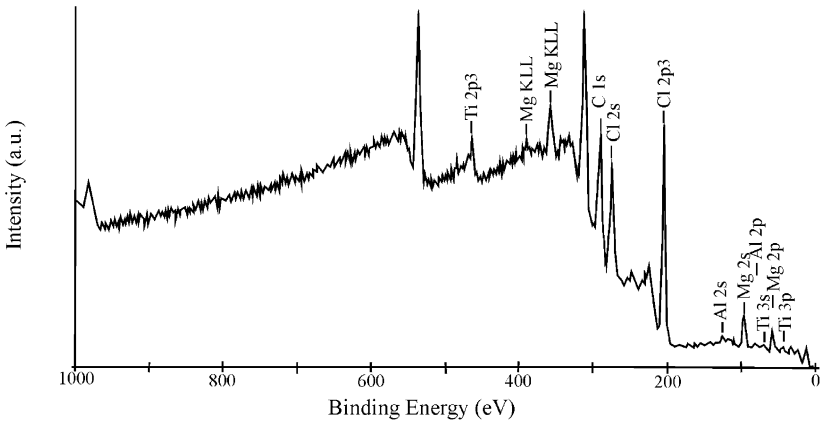

Fig. 4. XPS survey spectrum of ZNM24.

As expected, the Ziegler–Natta catalyst does not present any absorption band in the UV–VIS region (Fig. 3c). However, the hybrid catalysts, ZNM21 and ZNM24, presented absorption around 300 and 395 nm (Fig. 3d and e). That absorption maybe related to monoalkylated metallocene species in the hybrid catalysts generated on the $MgCl_2$ surface.

The XPS technique has been used to identify and quantify surface species, as well as to determine the binding energy of electrons in catalysts [44]. In this work, the nature of titanium present in the Ziegler–Natta, in the hybrid catalysts (ZNM21 and ZNM24) and in the Ziegler–Natta catalysts treated only with TIBA (ZNT1) was investigated. Fig. 4 shows a representative XPS survey spectrum (low resolution) of the hybrid catalyst (ZNM24). The constituent atoms of the Ziegler–Natta catalysts Mg, Cl, O, C, Ti were observed on the XPS surface spectrum as the Al from the co-catalyst.

Binding energy (BE) is not only related to the specific element, but contains chemical information of that environment, because the energy levels of core electrons depend on the chemical state of the atom. Chemical shifts are typically in the range 0–3 eV. Fig. 5 displays the Ti 2p core level spectra of the different titanium supported catalysts and the two signals in those are due to spin–orbit coupling of the 2p electrons of Ti: ca. 457 eV ($2p^{3/2}$) and 463 eV ($2p^{1/2}$). The Ti ($2p^{3/2}$) species of the $TiCl_4$ supported in the commercial Ziegler–Natta catalyst show a BE at 457.6 eV (Fig. 5a). After the Ziegler–Natta catalyst treatment with TIBA (Fig. 5b), this signal shifted to 458.8 eV, suggesting the generation of more electron deficient species, and the full width at half-maximum intensity (FWHM) increase, suggesting a broadening of these. The spectra deconvolution of the hybrid catalyst ZNM21 (Fig. 5c) shows that there are two Ti ($2p^{3/2}$) species, one centered at 457.6 eV related to $TiCl_4$ and a new one at 455.5 eV related to (Cp(*i*-Bu)$TiCl_2$). Similar spectrum was also obtained in the case of ZNM24 (Fig. 5d) presenting also two peaks: 457.4 and 455.1 eV. The low BE peak is observed in hybrid catalyst, due to the immobilization of (Cp)(*i*-Bu)$TiCl_2$ in the commercial Ziegler–Natta catalyst, suggesting the existence of Ti species in a richer electronic environment. Taking into account the Ti ($2p^{3/2}$) signal, when the amount of $CpTiCl_3$ in the catalyst preparation (ZNM24) was increased, a decrease in the Ti BE was observed, from 455.5 to 455.1 eV, that means an increase in electronic donation to Ti atoms and a broadening of the signal (higher heterogeneity in the nature of the surface species). On the other hand, a spectra deconvolution for the Ziegler–Natta commercial and ZNT1 catalysts was not observed, even for the ZNT2 catalyst, and since this was observed for the ZNM21 and ZNM24 spectra, the peak at lower BE can be attributed to the metallocene compound in the Ziegler–Natta catalyst.

Based on those results, we propose that the titanocene species Cp(*i*-Bu)$TiCl_2$ on the $MgCl_2$ surface are an alkylated species free of aluminium compound (Scheme 2). Although not represented, Al species

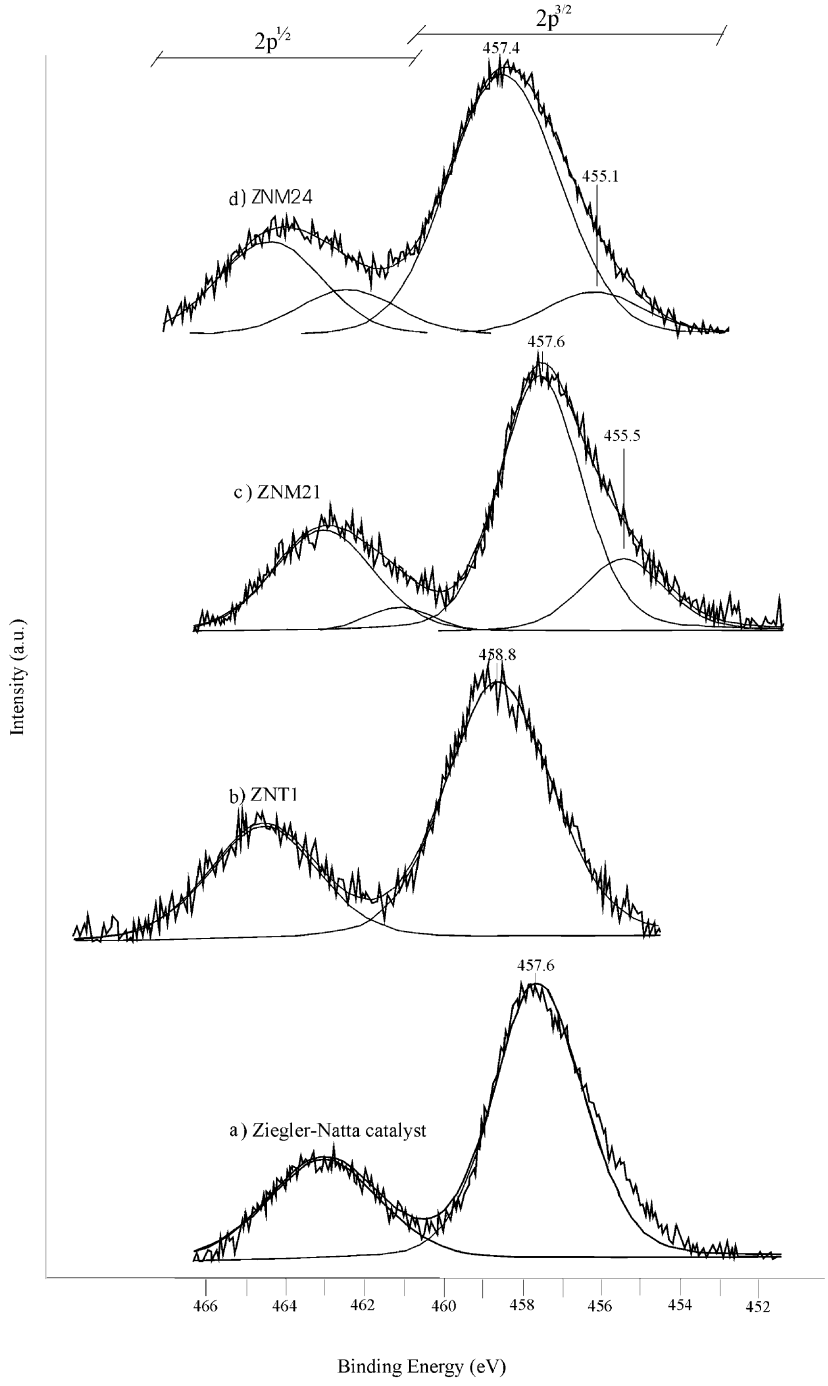

Fig. 5. High resolution XPS of Ti core region. (a) Ziegler–Natta catalysts; (b) ZNT1; (c) ZNM 21; (d) ZNM24. The small inserted peaks are the curve fit components, which are summed to obtain the smooth drawn line. The line with a visible noise component is the experimental raw data.

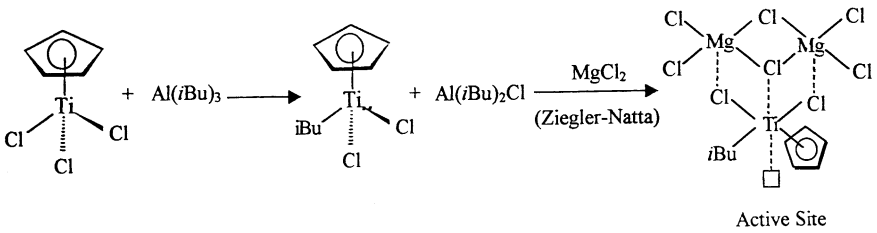

Scheme 2.

might be adsorbed on the $MgCl_2$ surface. The low Al/Ti ratio employed in the catalyst preparation might be enough to alkylate the titanium species, but it is not in excess to generate cationic surface species. The Al compound must be fixed on the $MgCl_2$ by replacing the internal donor (DIBP) as already discussed in the literature [45–50].

All the supported catalysts were evaluated in the copolymerization of ethylene-1-butene at Al/Ti molar ratio of 200 and 1000. The resulting polymers were

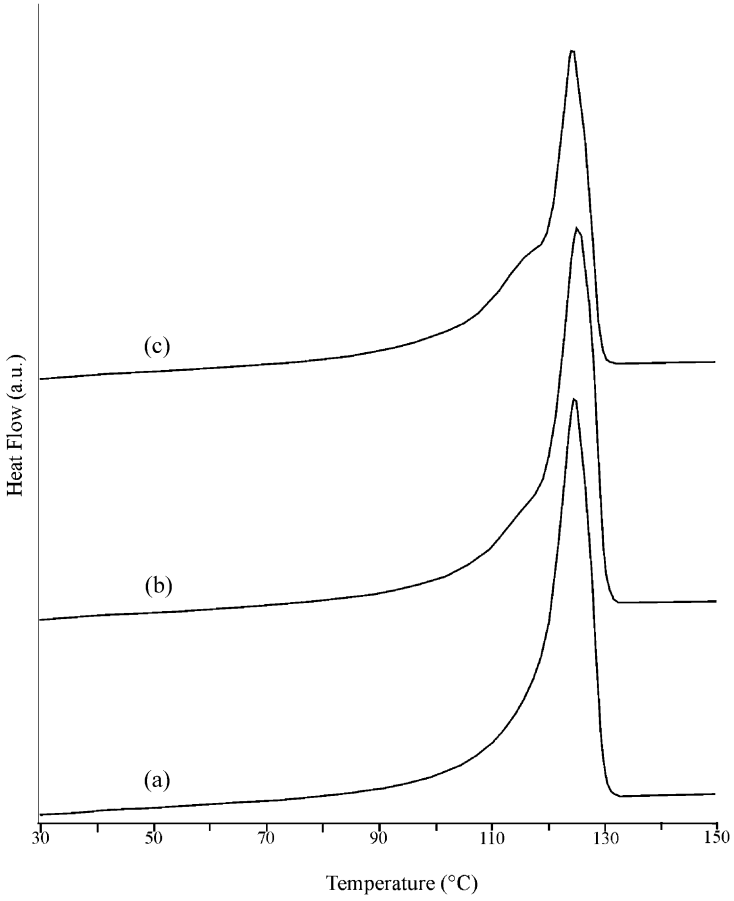

Fig. 6. DSC thermogramme of LDPE produced by (a) Ziegler–Natta catalyst; (b) ZNM21; (c) ZNM24.

Table 4
Catalytic activity in ethylene-1-butene copolymerization and melt flow index, melt flow ratio and comonomer content of produce polymers

	Catalyst	Al/Ti (molar ratio)	Activity (kg/g_{cat} h)	MFI (g/10 min)	MFR[a]	C_4 (%)
1	ZNM21	200	3.1	0.7	37.9	3.7
2	ZNM21	1000	7.0	2.2	32.0	4.6
3	ZNM24	200	5.7	0.2	44.0	3.0
4	ZNM24	1000	8.1	4.0	28.5	5.9
5	Ziegler–Natta	1000	8.6	1.7	33.2	4.5

[a] Melt flow ratio (2.16 kg/21.6 kg). Copolymerization conditions (2 l Büchi reactor): *n*-hexane = 1 l, time = 120 min, $T = 75^{\circ}C$, $P_{H_2} = 28$ bar (0.5 l), [butene] = 59 g/l, $P_{ethylene} = 7$ bar.

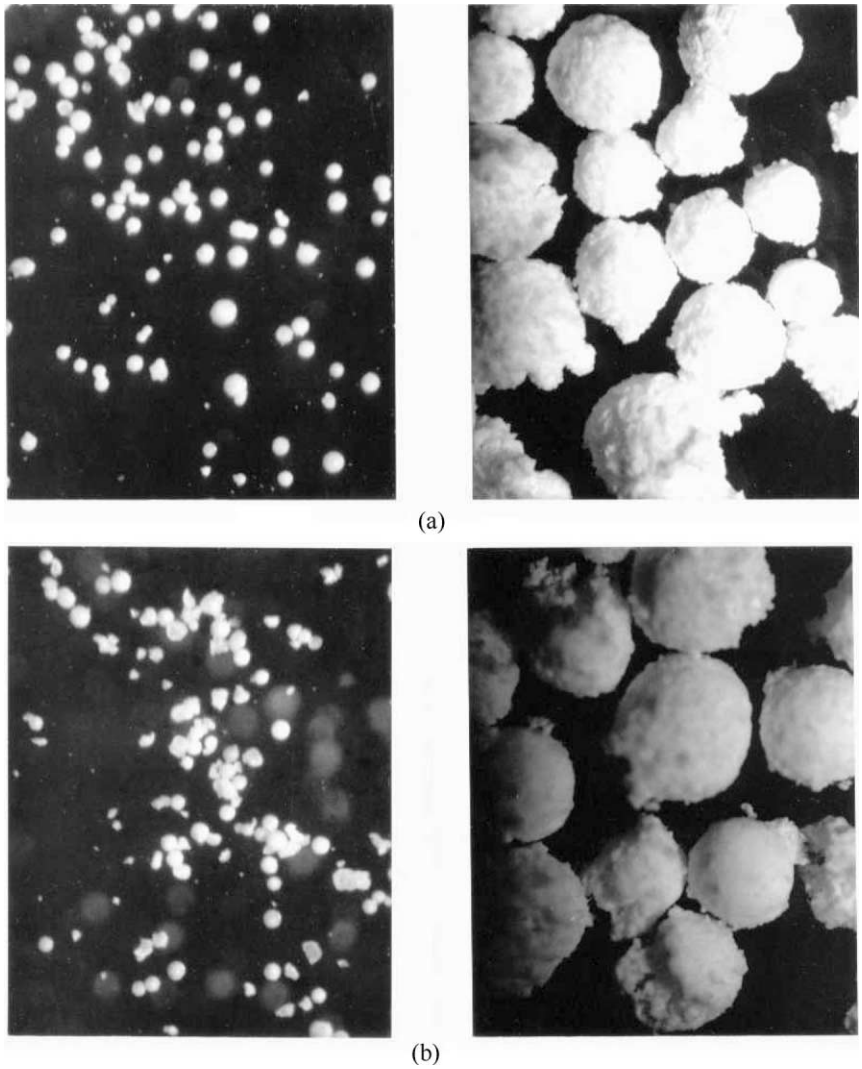

Fig. 7. Micrographs of catalyst (magnification, 100×) and resulting polymers (magnification, 16×) (a) Ziegler–Natta and (b) ZNM24 catalysts.

characterized by their melt flow index, melt flow ratio and comonomer incorporation (see Table 4). Both Ziegler–Natta and hybrid catalysts showed comparable catalyst activity at Al/Ti ratio equal to 1000. Only hybrid catalyst showed activity at Al/Ti molar ratio equal to 200. Comparing both hybrid catalysts, the one prepared with higher metallocene amount (ZNM24) showed the highest catalyst activity. Taking into account the Ti binding energy results from XPS (Fig. 5), it seems that the catalyst activity increases with decrease in BE Ti ($2p^{3/2}$) of both titanium species. Similar results were previously reported by Garbassi et al [51] in studying the activity of a series of homogeneous zirconocene catalysts with different ligands.

It was observed that the hybrid catalysts produced copolymers with higher MIF when compared with the Ziegler–Natta one, at Al/Ti molar ratio equal to 1000. Moreover, the comonomer incorporation was not significantly higher, at the same conditions. The polymer MFR obtained at Al/Ti molar ratio of 200 were higher than those obtained at 1000, that was very similar to those produced with Ziegler–Natta catalyst.

The DSC curves of LLDPE produced with the hybrid catalysts (ZNM24) (Fig. 6) showed a shoulder due to a crystallinity fraction not observed in the one produced with the Ziegler–Natta catalyst. This fraction happens to be due to the polymer chains with lower molecular weight or higher comonomer content produced by the active site (Cp(*i*-Bu)$TiCl_2$). This shoulder is more accentuated when a larger amount of metallocene is used in the catalyst preparation, due to the higher concentration of it.

Fig. 7 shows the micrographs of both catalyst and resulting polymers. It seems that the synthesis of the hybrid catalyst by modification of the Ziegler–Natta ones does not damage the latter's morphology (Fig. 7b). Besides, catalyst morphology was replicated during copolymerization of ethylene-1-butene with hybrid catalyst.

4. Conclusion

$MgCl_2$ supported Ziegler–Natta catalysts can be modified by metallocene ones producing a hybrid catalyst with new characteristics. The immobilization of (Cp)(*i*-Bu)$TiCl_2$ on Ziegler–Natta catalysts generates two Ti species on it, as observed by XPS measurements. The resulting hybrid catalysts showed activity in ethylene-1-butene copolymerization comparable to those of the Ziegler–Natta catalysts employed. The presence of a shoulder on the DSC thermogramme suggests the presence of two distinct sites when compared with the one produced with Ziegler–Natta catalyst. The polymer particles showed the replica of morphology phenomena.

Acknowledgements

This work was partially supported by the Brazilian Agency CAPES, and by OPP Petroquímica S.A (Triunfo, Brazil). We thank Japan Advanced Institute of Science and Technology (JAIST) for ^{27}Al MAS–NMR, UV–VIS, ICP–AES and XPS analyses.

References

[1] P. Corradini, V. Villani, G. Guerra, Macromolecules 18 (1985) 1041.
[2] V. Busico, P. Corradini, L. Martino, A. Proto, V. Savino, Macromol. Chem. 186 (1985) 1279.
[3] H. Mori, M. Terano, in: T. Sano, T. Uozumi, H. Nakatani, M. Terano, (Eds.), Progress and Development of Catalytic Olefin Polymerization, Technology and Education Publishers, Tokyo, 2000, p. 65.
[4] V. Busico, P. Corradini, A. Ferrara, A. Proto, Macromol. Chem. 187 (1986) 1115.
[5] V. Busico, Macromol. Chem. 187 (1986) 1125.
[6] V. Busico, Macromol. Chem. 191 (1991) 49.
[7] P. Corradini, V. Busico, R. Cipullo, Stud. Surf. Sci. Catal. 89 (1994) 21.
[8] W. Kaminsky, K. Külper, H. Brintzinger, F.R.W.P. Wild, Angew. Chem. Int. Ed. Engl. 24 (1985) 507.
[9] W. Kaminsky, J. Chem. Soc., Dalton Trans. 1413 (1998).
[10] B.A. Krentzel, Y.V. Kissin, V.I. Kleiner, L.L. Stotskaya, Polymers and Copolymers of Higher α-Olefins, Hanser Publishers, Munich, 1997, Chapter 1, p. 11.
[11] J.A. Ewen, Scientific American 5 (1997) 60.
[12] E. Gianetti, G. Nicoletti, R. Mazzocchi, J. Polym. Sci., Polym. Chem. 23 (1985) 2117.
[13] D. Cam, U. Giannini, Macromol. Chem. 193 (1992) 1049.
[14] G.G. Hlatky, H.W. Turner, R.R. Eckman, J. Am. Chem. Soc. 111 (1989) 2728.
[15] X. Yang, C.L. Stern, T.J. Marks, Organometallics 10 (1991) 840.
[16] J.C.W. Chien, W.M. Tsai, M.D. Rausch, J. Am. Chem. Soc. 113 (1991) 8570.
[17] M. Bouchmann, S.L. Lancaster, Angew. Chem. Int. Ed. Engl. 33 (1994) 1634.

[18] A.E. Hamielec, J.P.B. Soares, Prog. Polym. Sci. 21 (1996) 651.
[19] M.S. Ferrara, S.P. San Marco, G.G. Renazo, Montell Technology Company, Italy, USP 5698487, 1997.
[20] M.S. Ferrara, S.P. San Marco, G.G. Renazo, Montell Technology Company, Italy, USP 5759940, 1998.
[21] M.O. Jejelowo, Exxon Chemical Patents, USA, USP 5359015, 1994.
[22] A Razavi, Proceeding of ECOREP, 3–6 July 2000, Lyon, France.
[23] P. Kittilsen, T. McKenna, H. Svendesen, Proceeding of ECOREP, 3–6 July 2000, Lyon, France.
[24] G.G. Hlatky, Chem. Rev. 100 (2000) 1347.
[25] H.T. Ban, T. Arai, C.-H. Ahn, T. Uozumi, K. Soga, Currents trends in polymer science 4 (1999) 47.
[26] M.R. Ribeiro, A. Deffieux, M.F. Portela, Ind. Eng. Chem. Res. 36 (1997) 1224.
[27] J.D. Kim, J.B.P. Soares, G.L. Rempel, J. Polym. Sci., Polym. Chem 37 (1999) 331.
[28] E.S. Shamshoum, C.G. Bauch, US Patent 5,847,059 (1998); Chem. Abstr. 129 (1998) 95833.
[29] E.S. Shamshoum, M. Lopez, T.G. Harris, S. Kim, Eur. Pat. Appl. (1998); Chem. Abstr. 129 (1998) 276513.
[30] H.S. Cho, J.S. Chung, W.Y. Lee, J. Mol. Catal. A: Chem. 152 (2000) 215.
[31] F. Lopez-Linares, A. Daz Barrios, H. Ortega, J.O. Matos, P. Joskowicz, G. Agrifoglio, J. Mol. Catal. A: Chem. 152 (2000) 273.
[32] J.H.Z. dos Santos, S. Dorneles, F.C. Stedile, J. Dupont, M.C. Forte, I.J.R. Baumvol, Macromol. Chem. Phys. 198 (1997) 3529.
[33] J.H.Z. dos Santos, A. Larentis, M.B. da Rosa, C. Krug, I.J.R. Baumvol, J. Dupont, F.C. Stedile, M.C. Forte, Macromol. Chem. Phys. 200 (1999) 751.
[34] J.H.Z. dos Santos, C. Krug, M.B. da Rosa, F.C. Stedile, J. Dupont, M.C. Forte, J. Mol. Catal. A: Chem. 139 (1999) 199.
[35] J.H.Z. dos Santos, P.P. Greco, F.C. Stedile, J. Dupont, J. Mol. Catal. A: Chem. 154 (2000) 103.
[36] J.H.Z. dos Santos, H.T. Ban, T. Teranishi, T. Uozumi, T. Sano, K. Soga, J. Mol. Catal. A: Chem. 158 (2000) 559.
[37] D. Coevoet, H. Cramail, A. Deffieux, Macromol. Chem. Phys. 199 (1998) 1451.
[38] A.G. Potapov, V.V. Terskikh, G.D. Bukatov, V.A. Zakharov, J. Mol. Catal. A: Chem. 158 (2000) 457.
[39] A.G. Potapov, V.V. Terskikh, G.D. Bukatov, V.A. Zakharov, J. Mol. Catal. A: Chem. 145 (1999) 147.
[40] A.G. Potapov, V.V. Terskikh, G.D. Bukatov, V.A. Zakharov, J. Mol. Catal. A: Chem. 122 (1997) 61.
[41] M. Terano, T. Katoka, T. Keii, in: T. Keii, K. Soga (Eds.), Catalitic Polimerization of Olefins, Elsevier, Amsterdam, 1986, p. 407.
[42] M. Terano, T. Katoka, Macromol. Chem. 188 (1987) 1477.
[43] J. Kim, K.H. Kim, J.C. Cho, S. Kwak, K.U. Kim, W.H. Jo, H.S. Yoon, D.S. Lim, J. Polym. Sci. A: Polym. Chem. 36 (1998) 1733.
[44] T.L. Barr, Modern ESCA, The Principles and Practice of X-Ray Photoelectron Spectroscopy, CRC Press, Boca Raton, USA, 1994.
[45] P. Galli, P.C. Barbé, L. Noristi, Angew. Macromol. Chem. 120 (1984) 73.
[46] J.C.W. Chien, J.C. Wu, J. Pol. Sci., Pol. Chem. Ed. 20 (1982) 2461.
[47] V.A. Zaharov, S.I. Makhtarulin, V.A. Polyboyarov, V.F. Anufrienko, Macromol. Chem. 185 (1984) 1781.
[48] N. Kashiwa, J. Yoshitake, Polym. Bull. 11 (1984) 489.
[49] J.C.W. Chien, J.C. Wu, J. Pol. Sci., Pol. Chem. Ed. 21 (1983) 725.
[50] H.M. Park, W.Y. Lee, Eur. Polym. J. 28 (1992) 1417.
[51] F. Garbassi, L. Gila, A. Proto, J. Mol. Catal. A: Chem. 101 (1995) 199.